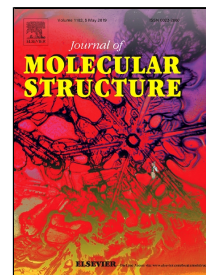


# Accepted Manuscript

Synthesis, single crystal X-ray structure and vibrational spectroscopic characterization study of a new hybrid material crystal: Bis(2,4,6-trihydroxy-1,3,5-triazin-1-ium) bischloride monohydrate



Hakima Chenefa AitYoucef, Riadh Bourzami

PII: S0022-2860(19)30309-6  
DOI: 10.1016/j.molstruc.2019.03.039  
Reference: MOLSTR 26308  
To appear in: *Journal of Molecular Structure*  
Received Date: 06 December 2018  
Accepted Date: 13 March 2019

Please cite this article as: Hakima Chenefa AitYoucef, Riadh Bourzami, Synthesis, single crystal X-ray structure and vibrational spectroscopic characterization study of a new hybrid material crystal: Bis(2,4,6-trihydroxy-1,3,5-triazin-1-ium) bischloride monohydrate, *Journal of Molecular Structure* (2019), doi: 10.1016/j.molstruc.2019.03.039

This is a PDF file of an unedited manuscript that has been accepted for publication. As a service to our customers we are providing this early version of the manuscript. The manuscript will undergo copyediting, typesetting, and review of the resulting proof before it is published in its final form. Please note that during the production process errors may be discovered which could affect the content, and all legal disclaimers that apply to the journal pertain.

**Synthesis, single crystal X-ray structure and vibrational spectroscopic characterization study of a new hybrid material crystal: Bis(2,4,6-trihydroxy-1,3,5-triazin-1-ium) bischloride monohydrate**

Hakima Chenefa AitYoucef <sup>a,\*</sup>, Riadh Bourzami <sup>b</sup>

Département Enseignement de Base en Technologie, Faculté de Technologie, Université Ferhat Abbas, Sétif-1, Algeria.

<sup>b</sup> Emerged material unit, university of Setif, Setif 19000, Algeria.

\*Corresponding authors E-mail address: hakimaaityoucef@yahoo.fr; aityoucefhakima@univ-setif.dz (Hakima Chenefa AitYoucef).

riadh\_bourzami@hotmail.com (Riadh Bourzami).

### **Abstract**

A new hybrid material bis(2,4,6-trihydroxy-1,3,5-triazin-1-ium) bischloride monohydrate ( $2C_3H_4N_3O_3^+ \cdot 2Cl^- \cdot H_2O$ ) as a crystal has been synthesized and its structure was identified by single-crystal X-ray diffraction and studied by UV-Vis, FT-IR, FT-Raman and  $^1H$  NMR. The crystal of  $2C_3H_4N_3O_3^+ \cdot 2Cl^- \cdot H_2O$  belongs to monoclinic with  $C_{2/m}$  space group system with  $Z = 4$ ,  $a = 12.3845(9)$  Å,  $b = 17.6236(14)$  Å,  $c = 7.0260(5)$  Å and  $\beta = 115.341(2)^\circ$ . The UV-Vis spectrum shows that the compound is transparent in visible and UV near visible domains. The FT-IR, FT-RAMAN and  $^1H$  NMR spectra of the crystal were discussed on the basis of crystallographic structure and the results were coherent and provides spectroscopic evidence for the crystal formation. In addition, the thermal decomposition of  $2C_3H_4N_3O_3^+ \cdot 2Cl^- \cdot H_2O$  has been also studied by TGA/DTG and DSC techniques and reveals that the material has a good thermal stability with the melting point about 310 °C.

**Keywords:** melamine; X-ray diffraction; FT-IR; FT-Raman; TGA; DSC

### **1. Introduction**

Recent technological breakthroughs and the desire for new functions generate an enormous demand for novel materials. Nowadays, most of them that have already entered the market are elaborated and processed by using conventional soft based routes developed in the eighties. In recent years there has been great interest in the development of new solid energetic materials, especially propellants with low signatures. Crystal engineering has significant applications in the field of material science [1-18]. The

important role in construction of new crystals seems to be reserved for weak intermolecular interactions such as hydrogen bonds, desired properties for this class of compounds are a halogen free, nitrogen- and oxygen-rich molecular composition and high densities. The hybrid materials crystals containing s-triazine as organic part, give improved hydrolytic and thermal stability [19], those compounds are six-membered heterocyclic aromatic rings consisting of three carbon atoms and three nitrogen atoms, the ring s-triazine is “planar” compound with the potential to form both single and double protonated cations and to participate in extensive hydrogen bonding. Also, the triazine ring is fairly resistant to electrophilic substitution, however, it may readily undergo ring cleavage with nucleophiles and is very sensitive to hydrolysis by water and other hydroxyl- compounds to a lesser degree [20,21].

Moreover, s-triazine many of its derivatives are used as pharmaceutical products [22], herbicides or building blocks in the field of supramolecular and coordination chemistry [23,24].

From all s-triazine-based compounds, 2,4,6-triamino-1,3,5-triazine commonly known as melamine or cyanuramide is the most well known. Another important derivative is 2,4,6-trihydroxy-1,3,5-triazine better known as cyanuric acid. Melamine as well as their derivative can form hydrogen-bonded self-assemblies with specific surface structures, these assemblies have been used as surface templates in supramolecular chemistry [25-33]. It can be hydrolyzed via deamination reactions under strong acidic and alkaline conditions and form cyanuric acid (2,4,6-trihydroxy-1,3,5-triazine) [34,35]. Melamine, which has a unique structure and is known as an important raw material, is widely studied and used to form hybrid materials [36-43]. Those materials containing s-triazine moiety as organic part, give improved hydrolytic and thermal stability [44]. Recent development shows that the melamine is an interesting molecule in the field of crystal engineering [36-43,45-48]. They are an important class of compounds due to the broad variety of their applications: they have over the years been subjected to extensive investigation by several researchers for their nonlinear optical properties, and have become an important area of research to build supramolecular structures of molecules via plusieurs liaisons hydrogène.

In our previous papers the molecular hybrid materials  $4\text{C}_3\text{H}_8\text{N}_6^{2+} \cdot 2\text{C}_3\text{H}_7\text{N}_6^+ \cdot 5\text{HPO}_4^{2-} \cdot 4\text{H}_2\text{O}$  [43] and  $4\text{C}_3\text{H}_5\text{N}_3\text{O}_3^{2+} \cdot 2\text{C}_3\text{H}_4\text{N}_3\text{O}_3^+ \cdot 5\text{HPO}_4^{2-} \cdot 4\text{H}_2\text{O}$  [49] were synthesized using melamine as starting materials and studied. It was

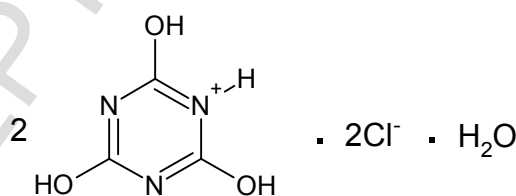
demonstrated that in all these crystals have a good thermal stability and very rich intermolecular hydrogen bonds.

Hence, as a continuation of our work on hybrid crystal based on s-triazine rings we have synthesized a new hybrid material crystal: Bis(2,4,6-trihydroxy-1,3,5-triazin-1-ium) bischloride monohydrate, further, the molecular structure were affined by single crystal X-ray diffraction and  $^1\text{H}$  NMR spectroscopy, various molecular vibration were assigned to the affined structure using FT-IR and FT-Raman spectroscopies, at the last, the thermal behavior was characterized by TGA/DTG and DSC techniques.

## 2. Experimental procedure

### 2.1. Synthesis and crystallization

The starting compounds, melamine (Aldrich, 99%) and hydrochloric acid (Aldrich, 37%) were used as supplied. The dissolved acid was added to the hot aqueous solution of melamine with the help of dropper, then the reaction mixture was brought to reflux under magnetic stirring. After 6 h of refluxing, the solution allowed to cool at room temperature, a white precipitate was formed, collected by filtration, then thoroughly washed with pure ethanol to remove the presence of impurities, and crystals were grown from aqueous solution using slow solvent evaporation process. The colorless and transparent crystals were formed during six days. Then, the chemical structure of the compound obtained (Scheme 1) was identified by single-crystal X-ray diffraction analysis.



Scheme 1. Chemical structure of  $2\text{C}_3\text{H}_4\text{N}_3\text{O}_3^+ \cdot 2\text{Cl}^- \cdot \text{H}_2\text{O}$ .

### 2.2 Characterization

The synthesized compound has been subjected to various characterization studies : single crystal X-ray diffraction, UV-Vis, FT-IR, FT-Raman and proton NMR. Wile, thermal analysis was performed by means TGA/DTG and DSC.

#### 2.2.1. Single crystal X-ray diffraction

A colorless single crystal of the of the compound  $2\text{C}_3\text{H}_4\text{N}_3\text{O}_3^+ \cdot 2\text{Cl}^- \cdot \text{H}_2\text{O}$  having the edges of  $0.45 \times 0.23 \times 0.14 \text{ mm}^3$  was mounted on a APEXII Bruker-AXS diffractometer for data collection, equipped with the graphite monochromator (MoK $_{\alpha 1}$  radiation source,  $\lambda = 0.71073 \text{ \AA}$ ) and  $\omega/2\theta$  scan mode with CCD detector, from: Center for Diffractometry (CDIFX), University of Rennes 1, France.

A crystal of good quality was selected its structure was solved by the direct methods using SHELXT (Sheldrick, 2015). Successive refinements based on F2 lead to a reliability factors of  $R = 0.048$ . Anisotropic thermal factors were determined for all non-hydrogen atoms. The hydrogen atoms were located from the difference Fourier maps and their positions and isotropic thermal parameters were refined.

The X-ray crystallographic data for the structure reported in this paper have been deposited at the “Cambridge Crystallographic Data Centre” (CCDC) according to the reference number 1484127.

#### 2.2.2. Spectroscopic measurements

The vibrational measurements were performed at room temperature. The UV–Vis spectral analysis was carried out in distilled water between 200–900 nm using a JASCO V-650 spectrophotometer with quartz cells of 1 cm path length. Fourier transform infrared (FT-IR) spectrum was taken on Perkin Elmer Spectrum one FT-IR spectrometer with the diffuse reflectance attachment (Miracle Attenuated Total Reflectance Attachment). Resolution was set up to  $4 \text{ cm}^{-1}$  resolution in the region  $4000\text{--}600 \text{ cm}^{-1}$ . FT-Raman spectrum was obtained on  $\mu$ -Raman type Labram confocal de Jobin-Yvon with a resolution of  $4 \text{ cm}^{-1}$  in the region  $3700\text{--}50 \text{ cm}^{-1}$ .  $^1\text{H}$  NMR spectrum of the synthesized compound was recorded using  $\text{DMSO-d}_6$  as solvent using  $\text{Me}_4\text{Si}$  (TMS) as internal standard on a Bruker Avance III 400 MHz spectrometer.

#### 2.2.3 Thermal analysis

Thermal behavior of  $2\text{C}_3\text{H}_4\text{N}_3\text{O}_3^+ \cdot 2\text{Cl}^- \cdot \text{H}_2\text{O}$  synthesized was provided in a simultaneous thermogravimetric analysis and differential thermal analysis (TGA–DTG) and a differential scanning calorimetry (DSC) cell. The temperature precision of the thermobalance and of the DSC cell was  $\pm 2$  and  $\pm 0.2 \text{ }^\circ\text{C}$  correspondingly instrument using a Perkin Elmer TGA 4000, under nitrogen atmosphere, with a heating rate of  $10 \text{ }^\circ\text{C}/\text{min}$  in the temperature range of over  $30\text{--}1000 \text{ }^\circ\text{C}$ .

### 3. Results and discussion

## 3.1. X-ray diffraction results

Details of the data collection parameters, crystallographic data and final agreement parameters are tabulated in Table 1.

Table 1. Crystal data, data collection and structure refinement details.

<i>Crystal data</i>	
Molecular	2C <sub>3</sub> H <sub>4</sub> N <sub>3</sub> O <sub>3</sub> <sup>+</sup> ·2Cl <sup>-</sup> ·H <sub>2</sub> O
Molecular	349.15 g.mol <sup>-1</sup>
Crystallin	Monoclinic <i>C</i> <sub>2/m</sub>
<i>D</i> <sub>x</sub>	1.702 Mgm <sup>-3</sup>
<i>Form</i>	Prism, colourless
Cell parameters	
<i>a</i>	12.3845 (9) Å
<i>b</i>	17.6236 (14) Å
<i>c</i>	7.0260 (5) Å
β	115.341 (2)°
T	150 K
Z	4
<i>V</i>	1385.93 (18) Å <sup>3</sup>
μ	0.51 mm <sup>-1</sup>
<i>F</i> (000)	736
<i>Data collection</i>	
<i>R</i> <sub>int</sub>	0.022
Radiation source	Mo( <i>K</i> α)
<i>h</i>	-16→15
<i>k</i>	-22→22
<i>l</i>	-6→9
θ <sub>max</sub> , θ <sub>min</sub>	27.5°, 3.2°
Measured reflections	4960
Independent reflections	1640
reflections with <i>I</i> >2.0σ( <i>I</i> )	1364
<i>Refinement</i>	
<i>R</i> [ <i>F</i> <sup>2</sup> > 2σ( <i>F</i> <sup>2</sup> )]	0.048
<i>wR</i> ( <i>F</i> <sup>2</sup> )	0.156
(Δσ) <sub>max</sub>	0.010
Δρ <sub>max</sub> , Δρ <sub>min</sub>	0.62, -0.68 eÅ <sup>-3</sup>
Parameters number	127

The asymmetric unit of title crystal is shown in Figure 1(a), it is made up by a two singly protonated at N atom of cyanuric acid (2CA<sup>+</sup>) cations, two chloride (2Cl<sup>-</sup>) anions and one water molecule, a research for structures containing (CA<sup>+</sup>) or (CA<sup>2+</sup>) yield are rare [49]. The cyanuric acid cations rings are distorted from ideal hexagonal form, the figure 1(b) shows the interatomic length and internal angle values of the triazine of one formal asymmetric unit, the difference can be explained by the lone pair electron steric effect, that is in a good agreement with the theory of the valence-shell electron pair repulsion (VSEPR) [50], also, it is seen one the same figure, that the triazine rings exhibit symmetry axes.

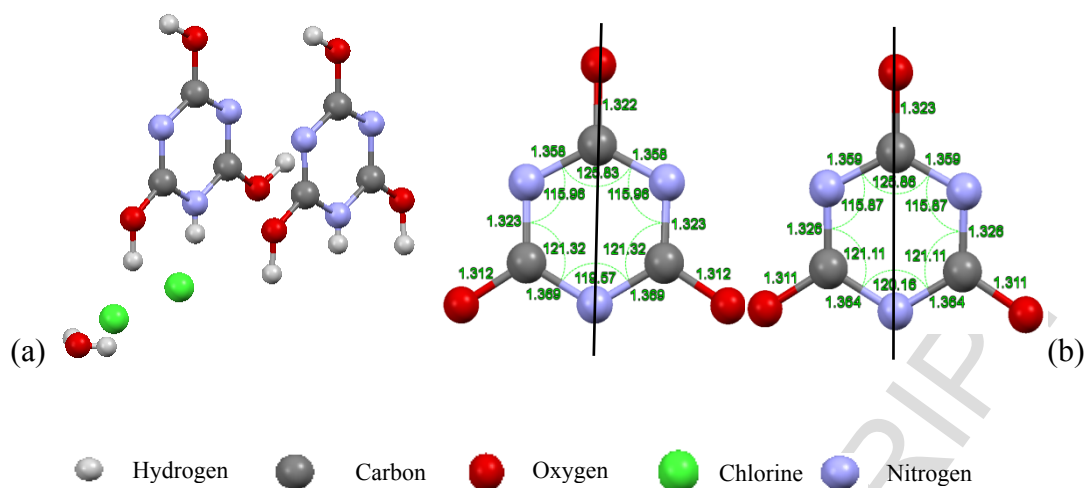


Figure 1. (a) asymmetric unit (b) geometry of s-triazine ring in the asymmetric unit.

Four asymmetric unit  $Z = 4$  form a monoclinic unit cell system (figure 2(a)), with  $C_{2/m}$  space group and the lattice parameters  $a = 12.3845(9) \text{ \AA}$ ,  $b = 17.6236(14) \text{ \AA}$ ,  $c = 7.0260(5) \text{ \AA}$  and  $\beta = 115.341(2)^\circ$ , in addition the unit cell is non-centrosymmetric, but characterized by two inversion centers at the positions  $(000)$  and  $(\frac{1}{4} \frac{1}{4} 0)$ , and also, a mirrors perpendicular to  $(010)$  planes. The crystalline structure is maintained principally by various intermolecular weak hydrogen bonds type, we compute 44 hydrogen bonds just in one unit cell, the first hydrogen bond type connects the organic and the inorganic parts of the compound and is of the type  $\text{OH}\cdots\text{O}$ , with donor acceptor length  $2.923 \text{ \AA}$ , observed between the hydroxyl group of the organic and the oxygen of water molecules of the inorganic parts, the second type is  $\text{NH}^+\cdots\text{O}$  between triazine rings, with donor acceptor length  $3.052 \text{ \AA}$ , those last form planar chain along  $(Oa)$  direction as shown in figure 2(b), moreover, along  $(Oc)$  direction the triazine rings form a stacking and creat an intermolecular interactions between parallel aromatic  $\pi$ -systems [51] (figure 2(c)) inducing a parallelism of the triazine chains. The last hydrogen bond maintains the inorganic part molecules of the type  $\text{OH}\cdots\text{Cl}^-$  between water molecules and charged chloride anions molecules, with two corresponding donor acceptor lengths  $3.156 \text{ \AA}$  and  $3.161 \text{ \AA}$ .

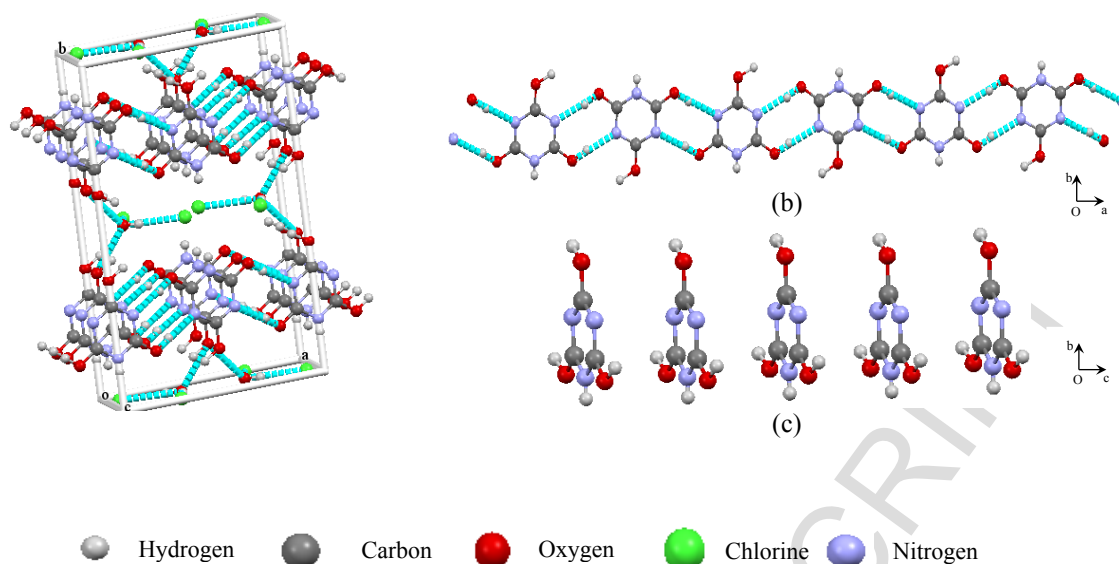


Figure 2. (a) unit cell with hydrogen bonds system (b) planar chain along (Oa) direction (c) staking of triazine rings along (Oc) direction.

Also, each chloride anions form four hydrogen bonds, relating two unit cells via lateral faces of the monoclinic system as shown in figure 3(a), two bonds of the type  $\text{OH}\cdots\text{Cl}^-$  in the same unit cell and the two authors of the type  $\text{NH}\cdots\text{Cl}^-$  with the adjacent unit cell, the corresponding donor acceptor lengths are  $3.257\text{\AA}$  and  $3.251\text{\AA}$  respectively. At the end, all hydrogen bond form a three dimensional layered network as shown in figure 3(b).

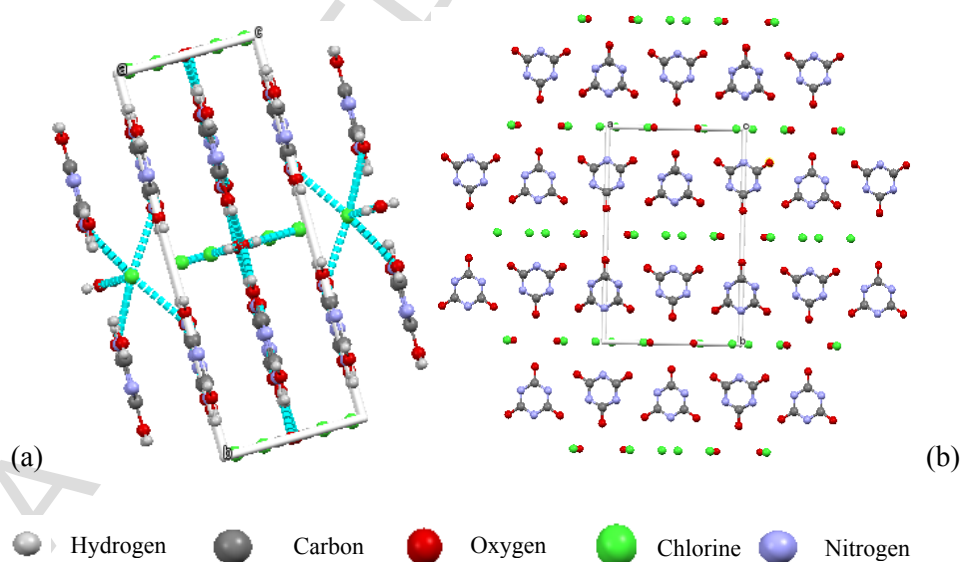


Figure 3. 3D network (a) Ocb view (b) Oab view.

### 3.2. Vibrational studies



### 3.2.1. UV-Vis

The electronic absorption spectrum of  $2\text{C}_3\text{H}_4\text{N}_3\text{O}_3^+\cdot 2\text{Cl}\cdot\text{H}_2\text{O}$  in distilled water (figure 4) proves that the crystal is transparent in the visible and UV near visible ranges. Moreover, two bands in the UV region are visible, maximized at 204.8 nm and 235 nm are assigned to  $\pi \rightarrow \pi^*$  and  $n \rightarrow \pi^*$  transition respectively.

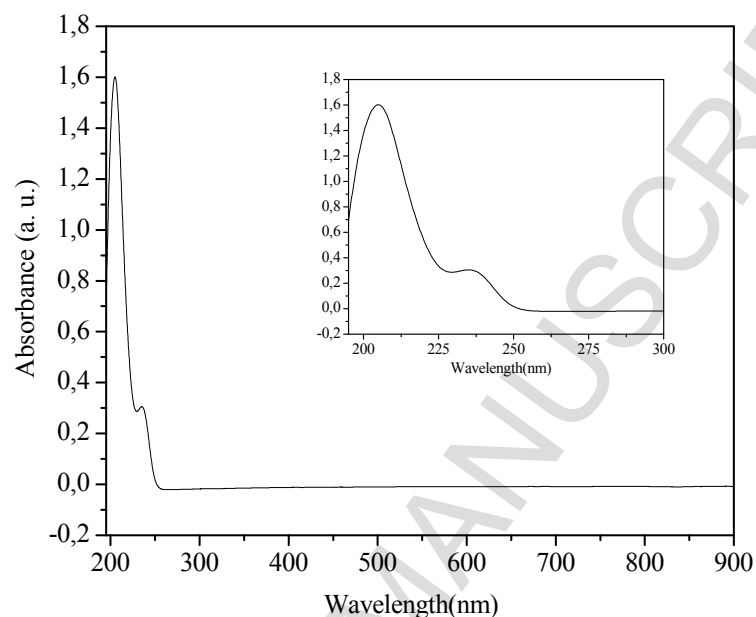


Figure 4. UV-Vis spectrum in distilled water.

### 3.2.2. FT-IR and FT-Raman studies

The bands observed in infrared and Raman spectra of  $2\text{C}_3\text{H}_4\text{N}_3\text{O}_3^+\cdot 2\text{Cl}\cdot\text{H}_2\text{O}$  are given in figures 5 and 6 respectively, arise from internal vibrations of single protonated cyanuric acid cations, chloride anions, the vibrations of water molecule and the vibrations of hydrogen bonds and from the vibrations of lattice. The significant infrared and Raman bands of the compounds synthesized are given in Table 2.

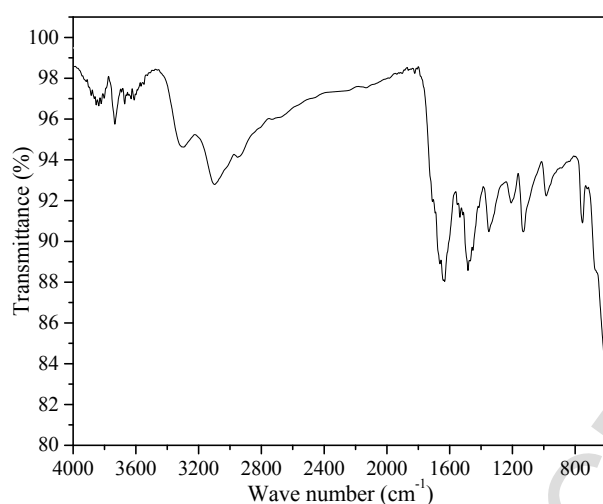


Figure 5. FT-IR spectrum.

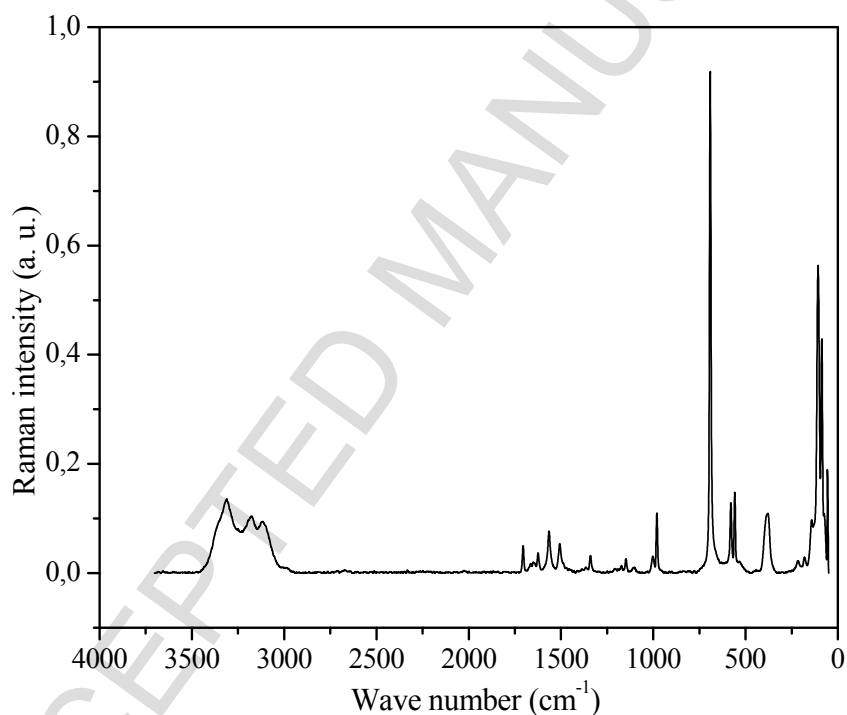


Figure 6. FT-Raman spectrum.

The FT-IR spectrum shows the disappearance of amine groups and appearance of new broad bands both originating from the vibrations of water molecule, as well as bands from the vibrations of OH groups of single protonated cyanuric acid cations are present in the region  $3700\text{--}3300\text{ cm}^{-1}$ , whereas the band observed at  $1649\text{ cm}^{-1}$  is assigned to the bending mode of OH. The Raman broad weak bands observed at  $3312$  and  $3181\text{ cm}^{-1}$  are assigned to  $\nu(\text{O-H})$  stretching and its bending at  $1623\text{ cm}^{-1}$ . Moreover, the hydrogen

bonds were appeared at  $3109\text{ cm}^{-1}$  in IR spectrum, and in Raman they were observed at  $3113\text{ cm}^{-1}$ . The IR bands corresponding to ring stretching vibrations appeared in the range  $1541\text{-}1370\text{ cm}^{-1}$ , and the weak bands at  $1146\text{ cm}^{-1}$  and  $999\text{ cm}^{-1}$  are assigned to triazine ring breathing mode of vibration [52]. Their weak Raman bands counterparts are seen at region  $1570\text{-}1360\text{ cm}^{-1}$ ,  $1150\text{ cm}^{-1}$  and  $1007\text{ cm}^{-1}$ . While the weak Raman bands located at  $983\text{ cm}^{-1}$  was due to triazine ring N in-plane radial type of vibration [53,54]. This peak usually occurs in between  $969\text{-}992\text{ cm}^{-1}$  and present in all melaminium [43,55], single protonated cyanuric acid ( $\text{CA}^+$ ) and doubly protonated cyanuric acid ( $\text{CA}^{2+}$ ) [49] it originates from the symmetric vibrations of s-triazine ring. The strong band at  $101\text{ cm}^{-1}$  is due to lattice vibration.

The strong intense peak at  $689\text{ cm}^{-1}$  is attributed to symmetric type of vibration of triazine ring [55] which is found in all melamine complexes [43,54-59] and singly or doubly protonated cyanuric acid [49]. Ring bending and ring quadrant out-of-plane were appeared at  $561\text{ cm}^{-1}$  [43,49,53] and  $379\text{ cm}^{-1}$  [43,49,54] respectively. All this assignment bands agree well with XRD analysis.

Table 2. FT-IR and FT-Raman vibrationnal wavenumbers ( $\text{cm}^{-1}$ ) and assignments.

FT-IR ( $\text{cm}^{-1}$ )	FT-Raman ( $\text{cm}^{-1}$ )	Assignments
3680		O–H stretching of water
3314	3312	O–H stretch of $\text{CA}^+$
	3181	O–H stretch of $\text{CA}^+$
3109	3113	Vibrations of hydrogen bonds O–H...O stretch
2956		O–H stretch $\text{CA}^+$
1675		$\text{H}_2\text{O}$ in plane bend
1649	1623	O–H Bending type of vibration
1541	1567	Ring: quadrant stretching; NCN bend
1500	1506	Ring: semi-circle stretch
1363	1341	C–O stretch
1216		C–OH in alcohol, C–O stretch
1146	1150	Ring: semi-circle stretch
999	1007	Triazine ring vibration breath
	983	Triazine ring N, in phase radial type of vibration
769		Ring sextant out of plane bending
	689	Symmetric type triazine ring
	585	Ring bending type of vibration
	561	Ring bending type of vibration
	379	Ring: sextant out-of-plane ben
	132	Lattice vibration
	101	Lattice vibration

### 3.2.3. $^1\text{H}$ NMR studies

According to the crystal structure, the  $^1\text{H}$  NMR spectrum of  $2\text{CA}^+ \cdot 2\text{Cl}^- \cdot \text{H}_2\text{O}$  (figure 7) exposed two singlets peaks at 7.85 ppm and 3.43 ppm are attributed to the –OH

of the mono-cyanuric acid cations and to water molecule respectively. Furthermore, The peak appeared at 2.50 ppm is due to the residual protons of deuterated  $\text{DMSO}_{d_6}$  solvent.

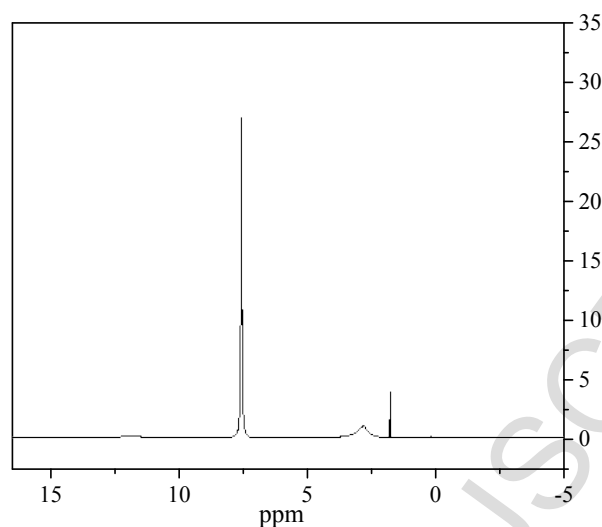


Figure 7.  $^1\text{H}$  NMR spectrum.

### 3.3. Thermal behavior

#### 3.3.1. Thermogravimetric studies

TGA/DTG curves recorded for the synthesized  $2\text{CA}^+ \cdot 2\text{Cl}^- \cdot \text{H}_2\text{O}$  is shown in figure 8.

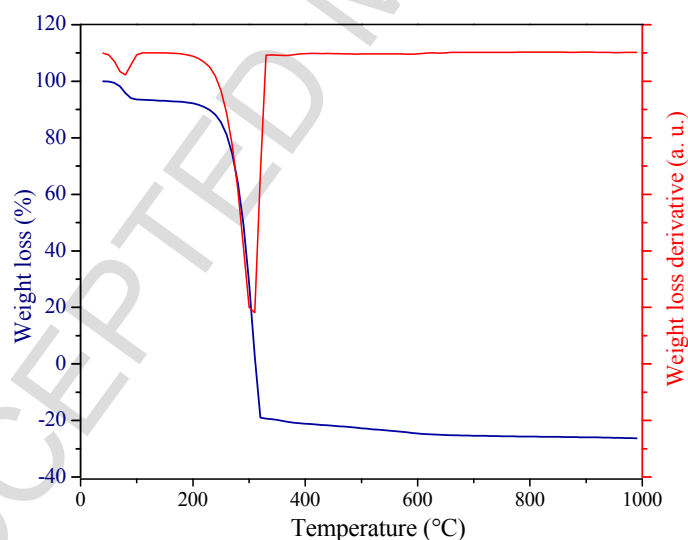


Figure 8. TGA curve (blue) and DTG curve (red).

TGA curve shows that this compound is stable until 207 °C. It is seen from the figure that the decomposition of  $2\text{CA}^+ \cdot 2\text{Cl}^- \cdot \text{H}_2\text{O}$  occurred in two stages involving dehydration and decomposition. There was mass loss of 5.23 % observed around 100°C which indicated the presence of water molecule in  $2\text{CA}^+ \cdot 2\text{Cl}^- \cdot \text{H}_2\text{O}$  was eliminated from

the structure, and the corresponding DTG peak was obtained at 80 °C. Whereas, the second stage of decomposition was accompanied by a rapid weight loss that take place in the temperature range of between 207 °C and 322 °C, with a weight loss of 94.77 %. There is a sharp weight loss presented on TGA curve, corresponding to a single peak at 310 °C on DTG curve suggest that there is no other processes of decomposition, except transition from solid to liquid state which is designated as melting point and this occurs at 310 °C as indicated in figure 8.

### 3.3.2. Differential scanning calorimetry (DSC) studies

The DSC was performed for the title crystal in the temperature range (30–1000 °C), the thermogram is shown in figure 9, and exhibits two endothermic peaks at 89 °C and 310 °C, those peaks are correlated with TGA analysis results.

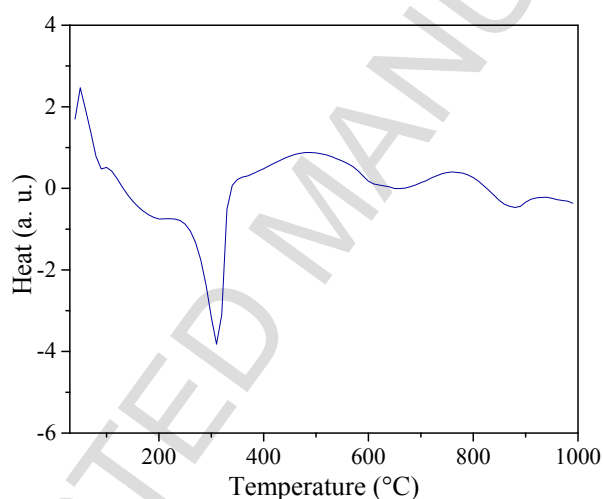


Figure 9. Differential scanning calorimetry curve.

## Conclusion

Bis(2,4,6-trihydroxy-1,3,5-triazin-1-ium) bischloride monohydrate  $2C_3H_4N_3O_3^+ \cdot 2Cl^- \cdot H_2O$  is a novel hybrid material was synthesized from the reaction of melamine and HCl, the corresponding crystals were grown from aqueous solution employing the technique of controlled evaporation, while its chemical structure was investigated by means of single crystal X-ray diffraction. The UV–Vis spectrum shows it has a good optical transmittance in the entire visible region. Vibrational spectroscopic FT-IR, FT-Raman and NMR analysis of the hybrid material are studied and are in the good agreement between spectroscopic and X-ray data is observed and confirms the structure of

the compound. From the thermal analysis, it is found that the melting point of the crystal was 310 °C, and shows thermal stability up to 207 °C. From this it is identified that this hybrid compound have more thermal stability and this enables the suitability of the crystal for thermal applications.

### Acknowledgements

The authors H. Chenafa AitYoucef and R. Bourzami would like to thank the Professor Lahcene Ouahab “Director of Research, CNRS, member of the European Academy of Sciences, Chemical Science Institute of Rennes, University of Rennes 1 and Doctor Thierry Roisnel for helping us in the crystallographic analysis.

### References

- [1] C. Sanchez, F. Ribot, Design of Hybrid Organic-Inorganic Materials Synthesized Via Sol-Gel Chemistry, *N. J. Chem.*, 18, 10, 1007, **1994**.
- [2] D. A. Loy, K. J. Shea, Bridged Polysilsesquioxanes. Highly Porous Hybrid Organic-Inorganic Materials, *Chem. Rev.*, 95, 5, 1431, **1995**.
- [3] C. Morterra, G. Magnacca, A case study: surface chemistry and surface structure of catalytic aluminas, as studied by vibrational spectroscopy of adsorbed species, *Catal. Today.*, 27, 3-4, 497, **1996**.
- [4] M. Lira-Cantu, P. Gomez-Romero, Electrochemical and chemical syntheses of the hybrid organic-inorganic electroactive material formed by phosphomolybdate and polyaniline. Application as cation-insertion electrodes, *Chem. Mater.*, 10, 3, 698, **1998**.
- [5] C. R. Kagan, D. B. Mitzi, and C. D. Dimitrakopoulos, “Organic-Inorganic Hybrid Materials as Semiconducting Channels in Thin-Film Field-Effect Transistors,” *Science*, vol. 286, no. 5441, pp. 945–947, **1999**.
- [6] E. Coronado, J. R. Galán-Mascarós, C. J. Gómez-García, and V. Laukhin, “Coexistence of ferromagnetism and metallic conductivity in a molecule-based layered compound,” *Nature*, vol. 408, no. 6811, pp. 447–449, **2000**.
- [7] C. Sanchez, G. J. A. A. Soler-Illia, F. Ribot, T. Lalot, C. R. Mayer, V. Cabuil, Designed Hybrid Organic-Inorganic Nanocomposites from Functional Nanobuilding Blocks, *Chem. Mater.*, 13, 10, 3061, **2001**.

- [8] D. B. Mitzi, "Thin-film deposition of organic-inorganic hybrid materials," *Chem. Mater.*, vol. 13, no. 10, pp. 3283–3298, **2001**.
- [9] E. Cordoncillo, P. Escribano, F. J. Guaita, C. Philippe, B. Viana, C. Sanchez, Optical properties of lanthanide doped hybrid organic-inorganic materials, *J. Sol-Gel Sci. Technol.*, 24, 2, 155, **2002**.
- [10] C. Sanchez, B. Lebeau, F. Chaput, J. P. Boilot, Optical properties of functional hybrid organic-inorganic nanocomposites, *Adv. Mater.*, 15, 23, 1969, **2003**.
- [11] F. Mammeri, E. L. Bourhis, L. Rozes, C. Sanchez, Mechanical properties of hybrid organic-inorganic materials, *J. Mater. Chem.*, 15, 35-36, 3787, **2005**.
- [12] C. Sanchez, B. Julian, P. Belleville, M. Popall, Applications of hybrid organic-inorganic nanocomposites, *J. Mater. Chem.*, 15, 35-36, 3559, **2005**.
- [13] W. Eerenstein, N. D. Mathur, and J. F. Scott, "Multiferroic and magnetoelectric materials," *Nature*, vol. 442, no. 7104, pp. 759–765, Aug. **2006**.
- [14] Y. Chen, L. Chen, G. Qi, H. Wu, Y. Zhang, L. Xue, P. Zhu, P. Ma, and X. Li, "Self-assembled organic-inorganic hybrid nanocomposite of a perylenetetracarboxylic diimide derivative and CdS," *Langmuir*, vol. 26, no. 15, pp. 12473–12478, **2010**.
- [15] M. Sessolo and H. J. Bolink, "Hybrid organic-inorganic light-emitting diodes," *Adv. Mater.*, vol. 23, no. 16, pp. 1829–1845, **2011**.
- [16] X. L. Wang, Y. L. Wang, W. K. Miao, M. B. Hu, J. Tang, W. Yu, Z. Y. Hou, P. Zheng, and W. Wang, "Langmuir and Langmuir–Blodgett Films of Hybrid Amphiphiles with a Polyoxometalate Headgroup," *Langmuir*, vol. 29, no. 22, pp. 6537–6545, **2013**.
- [17] H. Wang, H. Ohnuki, H. Endo, and M. Izumi, "Impedimetric and amperometric bifunctional glucose biosensor based on hybrid organic-inorganic thin films," *Bioelectrochemistry*, vol. 101, pp. 1–7, **2015**.
- [18] A. Kaushik, R. Kumar, S. K. Arya, M. Nair, B. D. Malhotra, and S. Bhansali, "Organic–Inorganic Hybrid Nanocomposite-Based Gas Sensors for Environmental Monitoring," *Chem. Rev.*, vol. 115, no. 11, pp. 4571–4606, **2015**.
- [19] K. Slimmer, P. Cristjanson, T. Kaljuvee, T. Pekh, I. Lasn, I. Saks, *J. Therm. Anal. Calorim.*, vol. 92, pp. 19-27, **2008**.
- [20] E. M. Smolin and L. Rapoport, *s-Triazines and Derivatives*. Interscience Publishers, Inc.: New York, 13, 644, **1959**.
- [21] J. M. E. Quirke, *Comprehensive Heterocyclic Chemistry*. Pergamon Press: Oxford, 3, 457, **1984**.

- [22]. Aksenov A. V., Aksenova, I. V. "Use of the ring opening reactions of 1,3,5-triazines in organic synthesis" *Chemistry of Heterocyclic Compds.* 45, pp 130-150, **2009**.
- [23]. K. Biradha and M. Fujita, A springlike 3D-coordination network that shrinks or swells in a crystal-to-crystal manner upon guest removal or re adsorption, *Angew. Chem. Int. Edit.*, 41, 3392-3395, **2002**.
- [24] P. Gamez and J. Reedijk, 1,3,5-Triazine-based synthons in supramolecular chemistry, *Eur. J. Inorg. Chem.*, 1, 29-42, **2006**.
- [25] Simanek, E. E.; Mammen, M.; Gordon, D. M.; Chin, D.; Mathias, J. P.; Seto, C. T.; Whitesides, G. M.; Design and synthesis of hydrogen-bonded aggregates. Theory and computation applied to three systems based on the cyanuric acid-melamine lattice *Tetrahedron*, 51, 607-619, **1995**.
- [26] Whitesides, G. M.; Simanek, E. E.; Mathias, J. P.; Seto, C. T.; Chin, D.; Mammen, M.; Gordon, D. M.; Noncovalent Synthesis: Using Physical-Organic Chemistry To Make Aggregates *Acc. Chem. Res.*, 28, 37-44, **1995**.
- [27] Li, X.; Chin, D. N.; Whitesides, G.M.; Synthesis and Evaluation of Thioether-Based Tris-Melamines as Components of Self-Assembled Aggregates Based on the CA·M Lattice; *J. Org. Chem.*, 61, 1779-1786, **1996**.
- [28] Mathias, J. P.; Simanek, E. E.; k, Jonathan A. Zerkowski; Christopher T. Seto; Whitesides, G.M.; Structural Preferences of Hydrogen-Bonded Networks in Organic Solution-the Cyclic CA·Ml "Rosette" *J. Am. Chem. Soc.*, 116, 4316-4325, **1994**.
- [29] Russell K. C.; Lehn J.-M.; Kyritsakas N.; DeCian, A.; Fischer J.; Self-assembly of hydrogen-bonded supramolecular strands from complementary melamine and barbiturate components with chiral selection; *J. New J. Chem.*, 22, 123-128, **1998**.
- [30] Philp, D.; Stoddart, J.F.; Self-Assembly in Natural and Unnatural Systems; *Angew. Chem. Int. Ed.*, 35, 1155-1196, **1996**.
- [31] Tanak, H.; Marchewka, M. K.; FT-IR, FT-Raman, and DFT computational studies of melaminium nitrate molecular-ionic crystal; *J. Mol. Struct.*, 1034, 363-373, **2013**.
- [32] Martin, A.; Pinkerton, A. A.; Melaminium Diperchlorate Hydrate; *Acta Cryst. C*, 51, 2174-2177, **1995**.



- [33] Choi, C. S.; Venkatraman, R.; Kim, E. H.; Hwang, H. S.; Kang, S. K.; Co-crystallization of melaminium levulinate monohydrate ;Acta Cryst. C, 60, 295-296, **2004**.
- [34] Janczak, J.; Perpetuo, G. J.; Bis (melaminium) DL-malate tetrahydrate; Acta Cryst. C, 59, 349-352, **2003**.
- [35] Janczak, J.; Perpetuo, G. J.;Melaminiumbis (4-hydroxybenzenesulfonate) dihydrate; Acta Cryst. C, 57, 873-875, **2001**.
- [36] Y. Wang, B. Wei, Q. Wang, J. Crystallogr. Spectrosc. Res., 20, 79, **1990**.
- [37] J.A. Zerkowski, G.M. Whitesides, J. Am. Chem. Soc., 116, 4298, **1994**.
- [38] R. Tanbug, K. Kirschbaum, A. Pinkerton, J. Chem. Crystallogr, 29, 45, . **1999**.
- [39] G.J. Perpetuo, J. Janczak, Acta Crystallogr., C58, o431, **2002**.
- [40] J. Janczak, G.J. Perpetuo, Acta Crystallogr. C60, o211, **2004**.
- [41] G.J. Perpetuo, J. Janczak, Acta Cryst. C62 ,o372–o375, **2006**.
- [42] Genivaldo Julio P., Jan Janczak, Supramolecular architectures in crystals of melamine and aromatic carboxylic acids J. Mol. Struct., vol. 891, 429–436, **2008**.
- [43] AitYoucef H.; Chafaa S.; Doufnoun R.; Douad T., Synthesis Characterizations and Thermal Behavior of Tetrakis (Melamine<sup>2+</sup>) Bis (Melamine<sup>+</sup>) Pentakis (monohydrogenphosphate) Tetrahydrate; J. Mol. Struct., vol. 1123, pp. 138–143, **2016**.
- [44] Lawrence, D. S.; Jiang, T.; Levett, M.; Self-Assembling Supramolecular Complexes Chem. Rev., 95, 2229-2260, **1995**.
- [45] A. Nangia, Curr. Opin. Solid State Mater. Sci. 5, 115–122, 2001.
- [46] L. Addadi, M. Geva, Crystal Eng. Commun. 5, 140–146, 2003.
- [47] O. Almarsson, M. Zwaorotoko, J. Chem. Commun. 17, 1889–1896, 2004.
- [48] J. Janczak, G.J. Perpetuo, Acta Crystallogr. C64, o91, 2008.
- [49] R. Bourzami; H. C. AitYoucef; N. Hamdouni; M. Sebais; Synthesis, crystal structure, vibrational spectra and thermal properties of novel ionic organic-inorganic hybrid material; Chem. Phys. Lett.; vol. 711, 220–226, **2018**.

- [50] Gillespie, R. P; The valence-shell electron-pair repulsion (VSEPR) theory of directed valency; *J. Chem. Educ.*, 40, 295-301, **1963**.
- [51] M.L. Głbwka, D. Martynowski, K. Kozłowska ; *Journal of Molecular Structure* 474, 81-89, **1999**.
- [52] W.J. Jones, W.J. Orville-Thomas, *Trans. Faraday Soc.* 55, 193–202, **1959**.
- [53] R.J. Meier, J.R. Maple, M.J. Hwang, A.T. Hagler, *J. Phys. Chem.* 99, 5445–5446, **1995**.
- [54] P.J. Larkin, M.P. Makowski, N.B. Colthoupe, The form of the normal modes of s-triazine: infrared and Raman spectral analysis and ab initio force field calculations, *Spectrochim. Acta A*55, 1011–1020, **1999**.
- [55] Y.L. Wang, A.M. Mebel, C.J. Wu, Y.T. Chen, C.E. Lin, J.C. Jiang, *J. Chem. Soc. Faraday Trans.* 93, 3445–3451, **1997**.
- [56] M.K. Marchewka, *Acta Chim. Solv.*, Infrared and Raman spectra and Raman spectra of melaminium bis (4-hydroxybenzenesulfonate) dihydrate, 50, 239–250, **2003**.
- [57] Y. Atalay, D. Avcı, A. Basoğlu, I. Okur, *J. Mol. Struct. (Theochem)* 713, 21–26, **2005**.
- [58] Y. Atalay, D. Avcı, *Spectrochim. Acta* 67A , 327–333, **2007**.
- [59] E. Tarcan, O. Altındag, D. Avcı, Y. Atalay, *Spectrochim. Acta* 71A, 169–174, **2008**.

**Highlights**

- New hybrid material  $2\text{C}_3\text{H}_4\text{N}_3\text{O}_3^+ \cdot 2\text{Cl}^- \cdot \text{H}_2\text{O}$  was synthesized.
- It crystallizes in monoclinic system with  $\text{C}_{2/m}$  space group.
- The cations are joined with anions and water molecule via hydrogen bonds.
- FTIR, FT-Raman and NMR studies of the compound were carried out.
- Thermal stability is up to 207 °C.